AN OBSERVATION OF HEAT BALANCE ON A SNOW FIELD AT THE TIME OF ABLATION IN 1963

Takuro SEO and Nobuyuki YAMAGUCHI

On the occasion of heavy snowfall in winter 1962/1963 in Hokuriku Region, the Suion-Chosakai (Institute for Water Temperature Research) organized a joint project for flood run-off due to snow-melting in the catchment area of Takinami River (a branch of Kuzuryu River) in March 1963. Our contribution to the program was the heat balance observation for the purpose of investigating the possibility of the estimate of snow-melting from meteorological data.

THE SITE AND PERIOD OF THE OBSERVATION

The observation point was situated on a flat school-playground on a slope facing south-east at Kitadani, Fukui Prefecture (N 36.1, E 133.6, height above MSL 375 m). The neighboring topography and the skyline viewed from the observation point is presented in Fig. 1 and Fig. 2 respectively.

The observation was carried out from 1800 March 25 to 1800 March 28, interrupted in the night of 27/28th. The weather was generally fair during the period before the cloud thickened in the afternoon of 28th and rain began in the evening. The depth of snow layer was about 190cm at the begining, decreasing to about 170cm at the end of the period. The course of snow depth in the period is shown in Fig. 3.

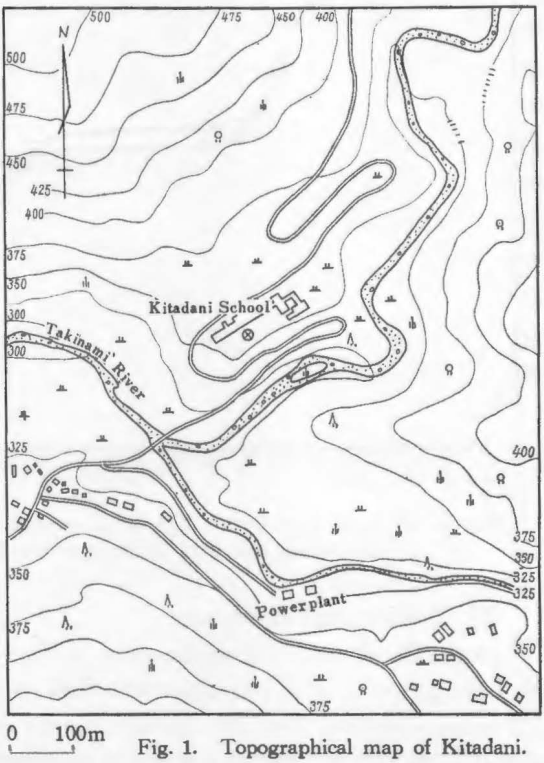

Fig. 1. Topographical map of Kitadani.
⊗: observation point

THE DETERMINATION OF THE COMPONENTS OF HEAT BALANCE ON THE SNOW SURFACE

Thermal exchange at the snow surface may be formulated as follows:

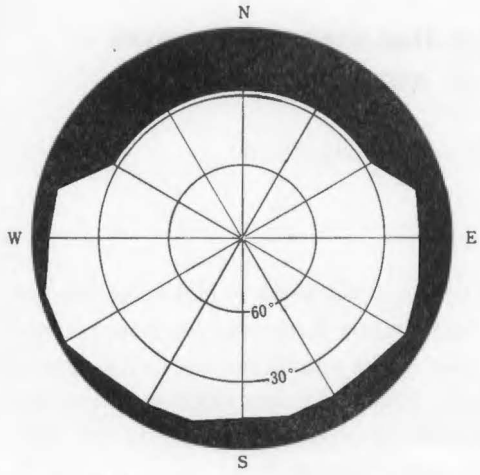

Fig. 2. Skyline viewed from observation point.

$$S = L + V + B + M$$

where S is the net radiation received at the snow surface, L the eddy transfer of sensible heat to the overlying air, V the latent heat loss by evaporation or sublimation, B the heat conduction into the snow layer, and M the heat available for snow-melting. In the present observation, S, L, V and B were mearured or calculated by the conventional methods (Literature 1—4) and M was obtained as the residual of the heat balance equation.

The observation were taken at interval of 1 hour in daytime and 3 hours in night, and each run was continued for about 10 minutes from the scheduled time.

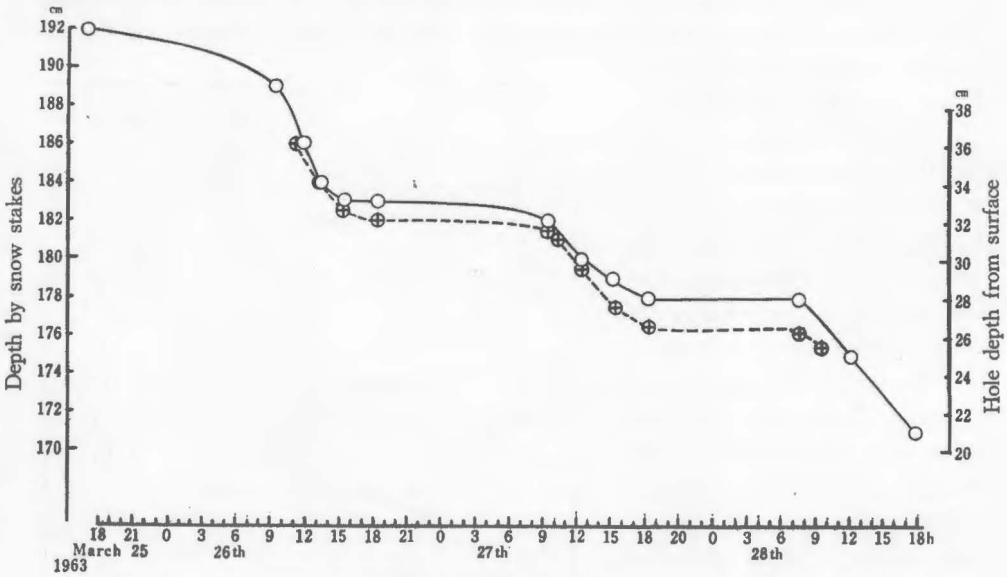

Fig. 3. Depth of snow layer. ○: depth measured by snow stakes, ⊕: depth of the cylindrical hole 2cm in diameter bored into the snow layer.

(1) *Radiational Exchange*

Net radiation received on the snow surface was measured by Albrecht's radiation balance meter, and its output was read by a millivoltmeter. Individual values of S were obtained from 30 readings for 10 minutes, and the mean values calculated from the individual values for successive 3 hours are shown in Table 1

TABLE 1

Three hours average of observed global radiation, total net radiation (S) and short-wave net radiation; long-wave net radiation and albedo determined from observed data; cloudiness

	Global radiation	Total net radiation	Short-wave net rad.	Long-wave net rad.	Albedo	Cloudiness
	(cal cm^{-2} min^{-1})					
March						
25—26th						
18—21h	0.01	−0.12	0.00	−0.12	—	1 Ac
21—0	0.00	−0.12	0.00	−0.12	—	0
0—3	0.00	−0.12	0.00	−0.12	—	0
3—6	0.02	−0.10	0.00	−0.10	—	0
6—9	0.36	0.06	0.17	−0.11	0.53	0
9—12	0.96	0.49	0.48	0.01	0.50	0
12—15	0.98	0.35	0.50	−0.15	0.49	0
15—18	0.33	0.00	0.16	−0.16	0.52	1 Ci
26—27th						
18—21h	0.00	−0.12	0.00	−0.12	—	0
21—0	0.00	−0.11	0.00	−0.11	—	0
0—3	0.00	−0.10	0.00	−0.10	—	2 Ci
3—6	0.01	−0.08	0.00	−0.08	—	6 Cs
6—9	0.32	0.12	0.15	−0.03	0.53	10 Cs
9—12	0.98	0.43	0.50	−0.07	0.49	5 Cs
12—15	0.92	0.36	0.48	−0.12	0.48	2 *
12—18	0.25	0.07	0.13	−0.06	0.48	2 *
28th						
6—9h	0.28	0.06	0.15	−0.09	0.46	7 *
9—12	0.97	0.41	0.50	−0.09	0.48	8 As
12—15	0.71	0.34	0.35	−0.01	0.51	10 As
15—18	0.08	0.07	0.04	0.03	0.50	10 As

The observed values of global radiation and short-wave net rediation are also shown in Table 1. Global radiation was measured by Gorczynski solarimeter, and short-wave net radiation was measured by a thermopile enclosed in the glass flask 6 cm in diameter placed at 50 cm above the snow surface. These elements were recorded by a multipoint recording potentiometer (ER 12—30, YEW), and the values at each observation time were obtained as averages from 10 points at interval of 1 minute.

These radiation instruments were standardized by Linke-Feußner actinometer (Actinometer CM 1, Kipp & Zonen).

Albedo on the snow surface can be calculated from the present data since the reflected short-wave radiation is obtained as the difference of observed global radiation and short-wave net radiation. The results given in Table 1 show that the albedo in the period was about 50 per cent and considerably small as compared with the one on the fresh snow surface.

The long-wave net radiation, which is given as the difference of net radiation and short-wave net radiation, is shown in Table 1. Average values for day and night are as follows:

March 25/26th	26th	26/27th	27th	28th
18—6h	6—18h	18—6h	6—18h	6—18h
−0.12	−0.10	−0.10	−0.07	−0.04

(cal cm^{-2} min^{-1})

We find that the radiative heat loss of about 0.1 cal cm^{-2} min^{-1} occured in the long-wave region through day and night in clear weather conditions. The average value obtained for 28th when the cloud thickened in the afternoon appeared small as compared with the values of the preceeding period. Detailed data shown in Table 1 indicate that the atmospheric long-wave radiation appeared to over-compensate the temperature radiation at the snow surface in the late afternoon of 28th.

(2) *Thermal Exchange between Snow Layer and Overlying Air*

The convective transfer of sensible heat to the overlying air L and the latent heat loss by evaporation or sublimation on the snow surface V were determined by the aerodynamic method, and Thornthwaite's expression was applied in the calculation:

$$L = \frac{C_p \rho k^2 (U_2 - U_1)(T_1 - T_2)}{(\ln Z_2/Z_1)^2}$$

$$V = \frac{\binom{600}{680} \rho k^2 (U_2 - U_1)(q_1 - q_2)}{(\ln Z_2/Z_1)^2}$$

where U_1, T_1, q_1; T_2, U_2, q_2 is wind velocity, air temperature and specific humidity at Z_1 and Z_2 height respectively, k Kármán's constant (0.4), ρ density of the air (1.25×10^{-3} g cm^{-3}), C_p specific heat of the air at constant pressure (0.24 cal g^{-1} deg^{-1}), $\binom{600}{680}$ latent heat of water by evaporation or sublimation (cal g^{-1}).

Observed data applied to the calculation are given in Table 2. Wind velocities at 150, 50 and 10 cm height were obtained from the numbers of revolution per 10 minutes of small cup anemometers, and air temperature and humidity at the corresponding levels by two Assmann psychrometers to ensure simultaneous observation at two levels.

In the further consideration of heat balance, the values of L and V calculated from the data observed at the lower levels are adopted, as these are considered to be less affected by the advection and the stability effect.

It is remarked that temperature inversion persisted through the period, and it was rather dominant in daytime as shown in Table 2. The vertical profile of vapor pressure, which was rather complex, showed in general a lapse condition in day and inversion in night. It is noticed that vapor pressure of the air exceeded

TABLE 2
Three hours average of observed wind velocity, air temperature and vapor pressure, and prevailing wind direction

	Wind velocity (cm/sec)			Air temperature (°C)			Vapor pressure (mb)			Wind direction
Height (cm)	150	50	10	150	50	10	150	50	10	
March										
25—26th										
18—21h	114	102	76	1.0	1.0	0.6	5.4	5.4	5.4	E
21—0	132	114	90	−0.3	−0.9	−1.4	4.4	4.6	4.4	E
0—3	128	112	84	−1.3	−2.0	−2.7	3.9	3.8	3.6	E
3—6	108	100	73	−2.0	−2.6	−3.3	4.2	4.0	3.6	ENE
6—9	107	89	69	0.9	0.7	0.1	4.2	4.1	4.2	W→E
9—12	111	90	66	7.9	7.8	6.7	4.1	4.2	4.8	WSW
12—15	102	79	58	10.8	10.0	8.8	3.4	3.6	5.2	WSW
15—18	129	110	84	8.5	7.7	6.8	4.4	4.7	5.3	W→E
26—27th										
18—21h	126	113	87	3.4	2.7	2.2	5.1	5.6	5.3	E
21—0	100	90	69	2.0	1.7	1.2	5.2	5.4	5.0	ENE
0—3	88	82	54	2.2	1.6	1.0	5.4	5.4	5.3	ENE
3—6	107	104	70	2.0	1.4	0.8	5.3	5.4	5.4	ENE
6—9	97	91	70	5.3	5.0	4.0	5.0	5.1	5.4	E→NW
9—12	95	(75)	55	10.7	10.2	9.3	4.5	4.6	4.9	W
12—15	120	98	73	13.3	12.6	11.5	*	4.0	4.7	SW
15—18	136	113	88	9.9	9.4	8.1	*	5.3	5.7	SW→E
28th										
6—9h	94	77	59	7.7	6.7	5.4	5.0	5.1	5.3	E
9—12	257	220	170	14.8	14.0	12.3	*	4.6	5.3	changeable
12—15	189	168	130	14.8	14.1	12.8	6.9	6.9	6.8	E
15—18	232	197	156	13.1	12.4	11.1	8.0	7.9	7.7	S~E

( ) estimated

the saturated values at the snow surface (6.11 mb) in the afternoon of March 28 with the falling weather.

(3) *Heat Conduction into the Snow Layer*

The heat conduction into the snow layer was determined by the method applied in the Artificial Snow-melting Project at Hirugano (4); it was obtained as the sum of heat storage in the 0—10cm layer and heat flux at 10cm depth. The former was calculated from the temperature change observed in the layer and the latter was measured by Albrecht's "Umsatzmesser". Relevant data are shown in Table 3 and Table 4.

TABLE 3

Snow temperature (T_S), density of 0—10cm snow layer (ρ) and water content by weight basis (w/m); and heat exchanged in 0—10cm snow layer $\left(\int_0^{10} C\rho \frac{\partial T_S}{\partial t} dZ\right)$

	Snow temperature (°C)			ρ	w/m(2)		$\int_0^{10} C\rho \frac{\partial T_S}{\partial t} dZ$(3)
	Surface	5cm	10cm	g cm^{-3}	%		(cal cm^{-2}/3h)
March 25—26th							
18h	−0.7	−0.1	(0.0)	0.32	13	25—26th	
21	−3.5	−0.2	(0.0)	*	*	18—21h	−1.4
0	−5.1	−0.4	−0.3	0.30	0	21— 0	−1.0
3	−7.7	−1.6	−0.2	*	*	0— 3	−1.8
6	−7.6	−2.6	−0.9	0.28	0	3— 6	−0.8
9	−0.9	−0.7	−0.2	0.36	14	6— 9	4.8
12	(0.0)	(0.0)	(0.0)	0.45	24	9—12	1.4
15	(0.0)	(0.0)	(0.0)	0.43	18	12—15	0.0
18	−0.2	(0.0)	(0.0)	0.41	8	15—18	0.0
26—27th							
18h	−0.2	(0.0)	(0.0)	0.41	8	18—21h	−1.4
21	−2.3	−0.2*	(0.0)	0.42	8	21— 0	0.2
0	−2.4	0.0*	(0.0)	*	7	0— 3	0.0
2	−2.4	−0.1*	(0.0)	0.39	0	3— 6	−1.2
6	−2.7	−1.1*	(0.0)	0.40	0	6— 9	2.5
9	(0.0)	(0.0)	−0.3	0.48	12	9—12	0.3
12	(0.0)	0.0	(0.0)	0.45	13	12—15	0.0
15	(0.0)	(0.0)	(0.0)	0.47	10	15—18	0.0
18	0.0	0.0	0.0	0.39	13		
28th							
6h	−2.7	−0.7	−0.4	0.44	0	6—9h	2.2
9	−0.3	0.0	−0.5	0.49	6	9—12	0.0
12	(0.0)	0.0*	(0.0)	0.50	21	12—15	0.0
15	(0.0)	0.0*	(0.0)	0.50	9	15—18	0.0
18	(0.0)	0.0*	(0.0)	0.55	10		

(1) Snow temperature was measured by thermocouple. * value by mercury thermometer adopted in the case of questionable indication of thermocouple.

(2) Water mass in sampled m g of snow.

(3) Specific heat of snow $C = \frac{w}{m} + 0.5\frac{m-w}{m}$

HEAT BALANCE ON THE SNOW SURFACE

S, L, V and B thus determined and M obtained as the residual of heat balance equation are tabulated in Table 5. From the table the results of observation are summarized as totals for day and for night:

TABLE 4

Temperature gradient $\left(\frac{\partial T_s}{\partial Z}\right)$, thermal conductivity ($\lambda$) and heat flux at 10cm in snow layer $\left(-\lambda \frac{\partial T_s}{\partial Z}\Big|_{z=10}\right)$ measured by Albrecht's "Umsatzmesser"

	$\frac{\partial T_s}{\partial Z}$ (°c/cm)	$10^4 \cdot \lambda$[1] (cgs)		$\left(-\lambda \frac{\partial T_s}{\partial Z}\Big|_{z=10}\right)$
March 25—26th			25—26th	
18h	0.0	1.7	13—21h	0.0
21	0.0	*	21— 0	0.0
0	0.05	1.5	0— 3	−0.1
3	0.05	*	3— 6	−0.1
6	0.05	1.2	6— 9	−0.1
9	0.15	*	9—12	−0.1
12	−0.05	1.7	12—15	0.0
15	0.0	*	15—18	0.0
18	0.0	1.8		
26—27th				
18h	0.0	1.8	26—27th	0.0
21	0.0	*	18—21h	0.0
0	0.0	*	21— 0	0.0
3	0.0	*	0— 3	−0.1
6	0.15	*	3— 6	−0.1
9	0.0	1.5	6— 9	0.0
12	0.0	*	9—12	0.0
15	(0.0)	1.8	12—15	0.0
18	0.0	2.3	15—18	
28th			28th	
6h	0.0	*	6— 9h	0.0
9	0.0	2.0	9—12	0.0
12	0.0	2.5	12—15	0.0
15	0.0	3.3	15—18	0.0
18	0.0	*		

(1) Table values are considerablly small as compared with the value cited in (5).

	25/26th 18—6h	26th 6—18h	26/27th 18—6h	27th 6—18h	28th 6—18h
			(cal cm^{-2}/12h)		
S	−83.7	162.2	−73.8	178.3	159.4
L	−11.7	−17.9	−12.1	−19.8	−43.0
V	− 7.1	20.3	− 7.3	13.9	8.3
B	− 5.2	6.0	− 2.5	2.7	2.2
M	−59.7	153.8	−51.9	181.5	191.9

The following results are of interest in the present observation:

1. Relatively large contribution of sensible heat flow L in the daytime (20—40 cal/cm²).

2. Prevalence of evaporation in the daytime (8—20 cal/cm²).

3. In the daytime sensible heat flow L is approximately compensated by evaporation V, and heat conduction into the snow is small in magnitude, so the value of radiational heat gain dominates the value of heat available for snow-melting. This may be taken as characteristic of the melting process in the fair weather conditions.

4. In 28th, sensibe heat flow to the snow increased, while evaporation decreased as compared with the preceeding fair days. Data given in Table 5 show that condensation began in the afternoon of 28th. It appeared that convective heat from the air to the snow takes an important part of snow-melting process when the warm and moist air flows over the snow layer.

5. Relatively large amount of negative M during the night as the latent heat

TABLE 5

Heat balance on the snow surface S: total net radiation, L: convective transfer of sensible heat, V: latent heat loss by evaporation or sublimation, B: heat condnction into the snow layer, M: heat available for snow-meltin ·.

	S	L	V	B	M
	(cal cm⁻² per 3 hours)				
March 25—26th					
18—21h	−21.6	− 1.6	0.0	−1.4	−18.6
21— 0	−22.5	− 2.3	−1.4	−1.0	−17.8
0— 3	−21.6	− 3.8	−2.4	−1.9	−13.5
3— 6	−18.0	− 4.0	−3.3	−0.9	− 9.8
6— 9	10.8	− 2.6	0.6	4.7	8.1
9—12	87.6	− 5.2	5.1	1.3	86.4
12—15	63.3	− 5.3	10.1	0.0	58.5
15—18	0.5	− 4.8	4.5	0.0	0.8
26—27th					
18—21h	−20.7	− 2.4	−2.8	−1.4	−14.1
21— 0	−19.8	− 1.8	−2.9	0.2	−15.3
0— 3	−18.0	− 3.4	−1.0	0.0	−13.6
3— 6	−15.3	− 4.5	−0.6	−1.3	− 8.9
6— 9	22.5	− 4.1	2.2	2.4	22.0
9—12	78.0	− 3.7	1.9	0.3	79.5
12—15	64.8	− 5.4	6.5	0.0	63.7
15—18	13.0	− 6.6	3.3	0.0	16.3
28th					
6— 9h	11.3	− 4.9	1.4	2.2	12.6
9—12	74.2	−17.6	10.1	0.0	81.7
12—15	60.8	− 9.6	−0.3	0.0	70.7
15—18	13.1	−10.9	−2.9	0.0	26.9

liberated in the freezing process in the surface layer of snow.

It is possible to estimate the ablation from the melting heat of snow M given above, taking account of snow density ρ and water content (w/m). The calculated ablation ($\triangle H_{comp}$) and the one observed by snow stakes ($\triangle H_{obs}$) are as follows:

March 1963		26th	27th (6—18h)	28th
snow melted $M'=M/80$	g/cm²	1.92	2.27	2.39
ablation computed $\triangle H_{comp}=M'/(1-w/m)$	cm	5.6	5.7	5.2
ablation observetd $\triangle H_{obs}$	cm	6	5—5.2	7

For the complete comparison, more detailed knowledge will be required about the structure of the snow layer. Agreement between calculated and observed values, however, shows that the application of the heat balance method is satisfactory to estimate the snow-melting.

LITERATURE CITED

(1) Sverdrup, H. U. 1936. The eddy conductivity of the air over a smooth snow field. Geof. Publ. XI, No. 7.

(2) Untersteiner, N. 1958. Grazial-meteorologische Untersuchungen in Karakorum II. Arch. Met. Geoph. Biokl. Ser. B, 8: 137.

(3) Ambach, W. 1961. Investigations of the heat balance in the area of ablation on the Greenland Ice Cap. Arch. Met. Geoph. Biokl. Ser. B, 10: 278.

(4) Kansai Electric Power Co. 1956. Jinko Yusetsu Jikken (Artificial snow-melting experiment) (June 1956).

Seo, T. 1957—1958. A microclimatological study of thermal exchange at the earth's surface. The Meteorological Notes of the Meteorological Research Institute, Kyoto University, Ser. 2, No. 17.

(5) Geiger, R. 1961. Das Klima der bodennahen Luftschicht. 4. Aufl. S. 220.